Testing fish freshness by using a mechanical probe

Chris Budd, Tim Myers, and R. Eddie Wilson

1 Introduction

A method for testing fish freshness proposed by Paul Nesvadba at the Food Research Institute at the Robert Gordon University, Aberdeen, is to use a mechanical 'fish probe'. This device is illustrated in Figure 1. It comprises a thin needle-like probe enclosed within a case in which there

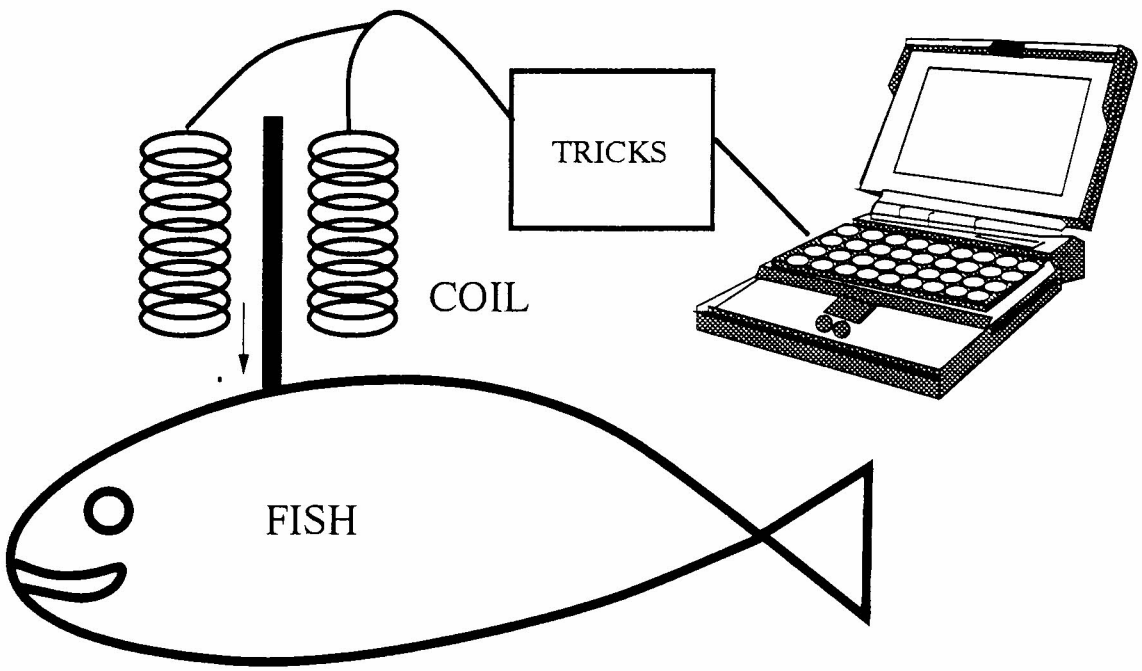

Figure 1: The experimental set-up.

is a coil. This coil acts both to give an electromagnetic force to the probe and also to measure the motion of the probe. Measurements from the coil can be recorded electronically and used for later analysis. The operation of the probe is as follows. The whole device is placed upon a fish so that the needle comes to rest on the skin of the fish under the force of gravity alone. A constant force F is then applied to the needle by passing a current through the coil. This force causes the probe to move toward the fish, depressing but not piercing the skin. The resulting motion of the probe can then be monitored over the time interval (in milliseconds) that it takes to reach equilibrium. In this time interval the intial motion is elastic (due to the behaviour of the skin of the fish) and later motion is governed by visco-elastic forces and is dominated by the motion of the fluid inside the fish. (An analysis of this latter motion is given in Section 2.) After the needle has reached equilibrium the force F is suddenly released. The needle then moves upwards as the skin of the fish and the fluid within the fish returns to its unperturbed state. The resulting motion is then monitored. It is unclear whether during this motion the needle always stays in contact with the skin of the fish, or whether it loses contact and starts to move in free fall. There is some evidence to support the latter hypothesis. (For an analysis of this motion, see Section 3.)

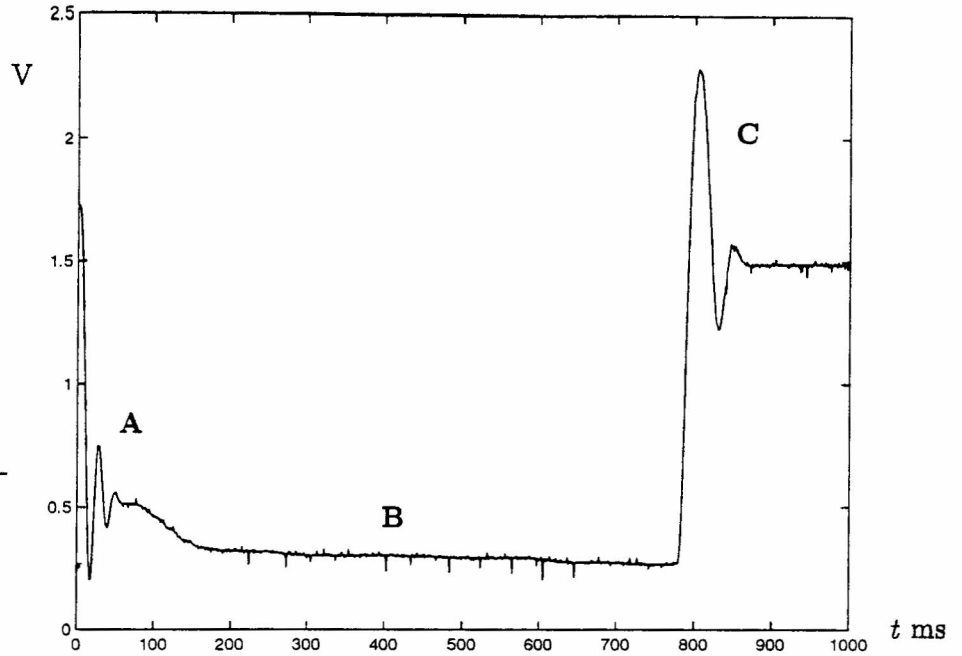

Figure 2: A typical graph produced by the probe: transducer output voltage against time.

The response of the probe was measured on various materials including some (fresh) fish purchased for the meeting (by Alan Zinober) and various human participants, both young and old. The measurements clearly showed a difference in the behaviour of the different materials, and indeed was effective in determining the approximate age of the humans tested. The overall response had the form shown in Figure 2. It comprises three main phases of evolution:

A Initial motion into the skin.

B Later motion as fluid is displaced.

C Final motion when the force is released.

Each of these responses gives information about the composition of the fish. The basic questions for the study group were

1. What information (fish dependent constants) could be extracted from the probe data?
2. How reliable are these measurements? Do they depend upon where on the fish the measurements are made, how firmly the probe is held, how sticky the fish skin is?
3. What, if anything, would the measurements tell us about freshness?

Phases A and B The simplest measurement of all is the total elastic drop Δ_1 when the force is applied to the skin of the fish. This drop could be measured as a voltage change in the coil to a reasonable level of accuracy. The following table gives results of tests on some different materials:

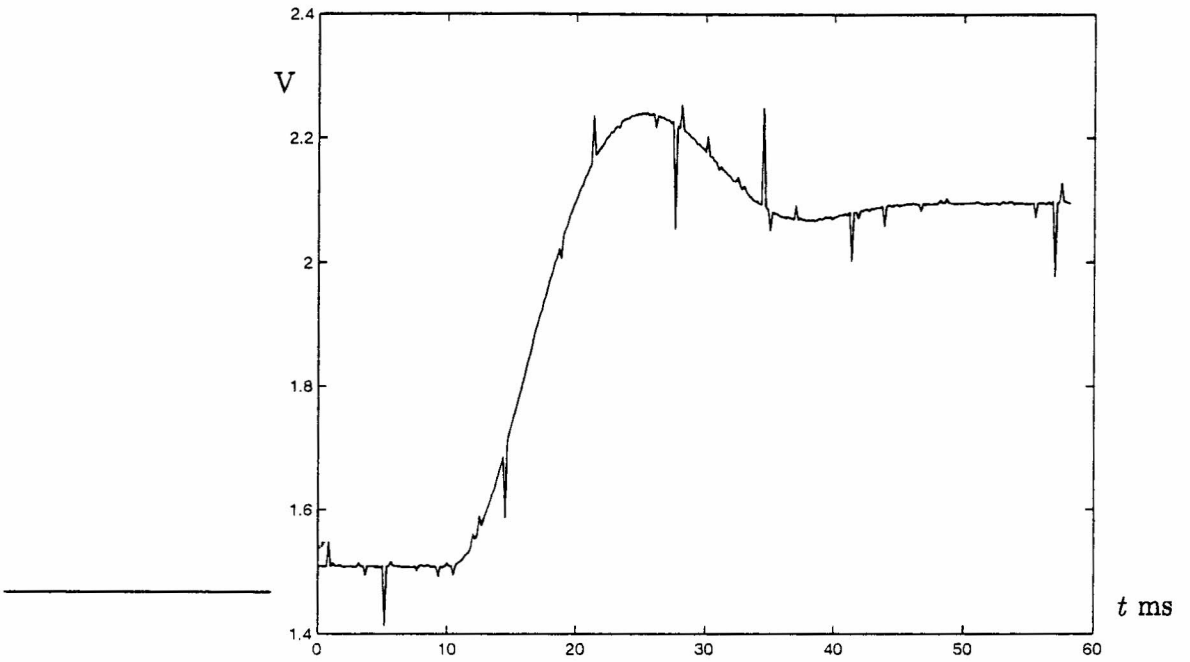

Figure 3: The phase C probe trace for a plaice head.

Fish	Δ_1/V
Mackerel	0.55
Trout head	0.7
Trout body	1.1
Plaice head	0.4
Plaice body	0.7
Cod fillet	0.25
Chris Budd's hand	0.4

A calibration test on the probe indicated that

$$1\text{mm} = 0.8\text{V}.$$

Note, under this measurement, Chris Budd is indistinguishable from a plaice head. See a further discussion of this result in [1]. Phases A and B are given a detailed analysis in Section 2.

Phase C Three responses of the probe after the force is released are given in Figures 3–5. In Figure 4 a very similar response is found when using a plaice side or elastic foam. To produce the last figure a simulated fish was produced by stretching cling film over a cup. In this experiment the response was purely elastic with no fluid motion. The resulting response is very similar to that measured on a cod.

To a first inspection the response of the plaice head looks like that of a heavily damped linear oscillator and that of the plaice side like a lightly damped linear oscillator. (A more detailed analysis will show that these descriptions are oversimplified). In contrast the response of the cod and of the cling film was very different and for topological reasons can not be described by saying that the motion was the solution of simple second order oscillator (either linear or nonlinear) but

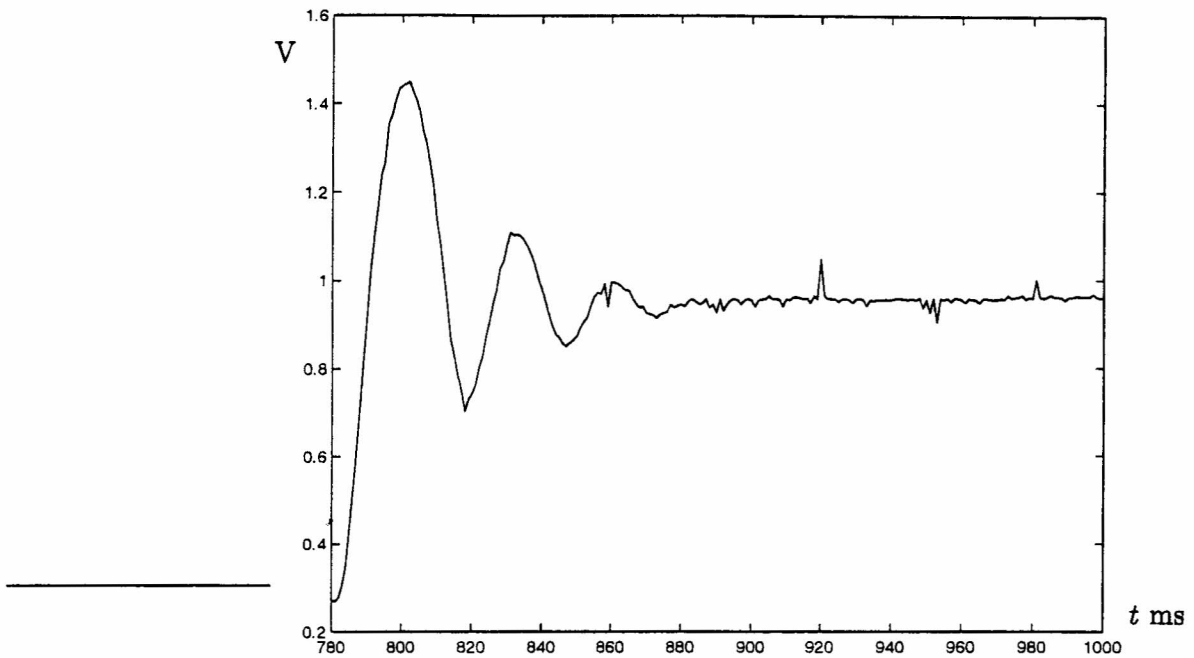

Figure 4: The phase C probe trace for a foam sample (which is very similar to a plaice side).

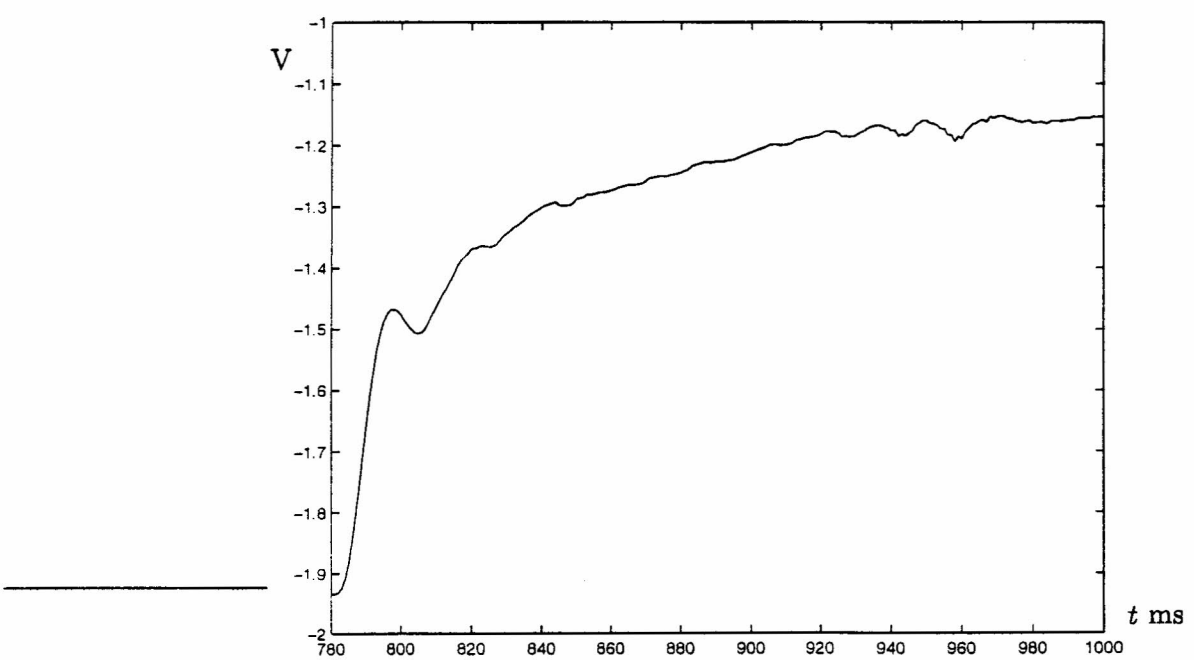

Figure 5: The phase C probe trace of cling film stretched over the opening of a polystyrene cup.

could in principle be modelled by a multi-modal oscilator. There is however, some evidence here that the needle may be losing contact with the skin or cling film as it accelerates upwards.
To summarise, a series of models of the probe

- Simple linear,
- Simple nonlinear,
- Multi-modal,
- Loss of contact,

were developed to explain the phase C motion. See Section 3 for details.

2 Models of the initial phases A and B: an approximate solution for the axisymmetric indentation of a fluid filled elastic porous media

All soft connective tissue in an animal body is composed primarily of three components; cells, extracellular matrix and interstitial water [2]. The cells and extracellular matrix together form an elastic porous solid, the interstitial water fills the pore spaces. Tissue may therefore be considered as a fluid filled deformable porous media. Media of this type have been studied extensively in biological applications [3, 4, 5]. An important, related engineering application is the consolidation of soil under a building, see [6, 7, 8] for example. Other relevant areas include irrigation, flow of saline through a water table, filtering and separation columns [5].

The problem of interest to the present study is the indentation of a porous media by a cylindrical indenter. This is also of practical interest in characterising oedema and consolidation of soil. Chiarella & Booker [8] discuss the consolidation of a cylindrical indenter on a deep clay layer. They state that the process occurs in three distinct stages. At sufficiently small times the displacements and stresses are the same as if the material were an incompressible elastic solid [9]. At sufficiently large times the behaviour is identical to a purely elastic, compressible solid. At intermediate times creep occurs as the fluid is forced out of the pore spaces. This fits exactly with the experimental results presented at the Study Group.

The following models are intended to describe the indentation of a fluid filled porous media by a small rigid indenter which is subject to a constant applied load. Results are first presented for the small and large time behaviour of an elastic half-space subjected to indentation by a cylindrical punch of radius a. A model is then developed for the flow of an incompressible inviscid fluid through an elastic porous media. The model is based on the biphasic theory of Mow *et al* [4], which in turn is based on the poroelastic theory of soil mechanics [7, 8]. Finally, a simple one-dimensional model for the deformation of a viscoelastic solid is presented. This solution is shown to have the same qualitative behaviour as the more complex porous media model. In particular, the deformation is characterised by a single constant which combines the elastic and viscous responses of the material.

Due to time constraints a mixture of axisymmetric and one-dimensional models are presented. Clearly this is not an ideal situation, particularly when comparing models, but it does permit a number of simple analytical results to be obtained and paves the way for subsequent, more thorough investigations.

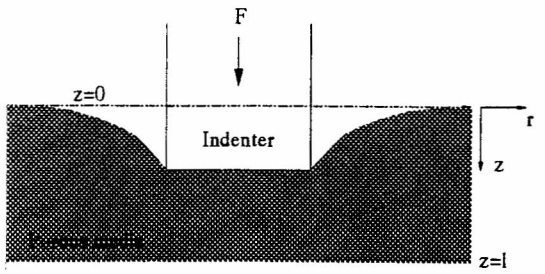

Figure 6: An axisymmetric indenter on a porous media.

2.1 Short and large time elastic response

At sufficiently large times all the fluid occupying the pore spaces will have redistributed and attained its equilibrium pressure (which may be set to zero). The deformation at this time is purely elastic. Provided the indentation depth is small compared to the overall thickness of the tissue layer, the classical solution of Boussinesq for the indentation of an elastic half-space may be applied, see [10] for example. This specifies the final indentation of the punch as

$$w_\infty = \frac{(1-\nu^2)F}{2aE}\,, \tag{2.1}$$

where F is the applied force, ν is Poisson's ratio and E is the Youngs modulus. As mentioned in the introduction, the small-time deflection corresponds to the solution for an incompressible elastic material. The initial deformation is therefore obtained by substituting $\nu = 1/2$ into equation (2.1):

$$w_s = \frac{3F}{8aE}\,. \tag{2.2}$$

The two deformations, w_s and w_∞, are measurable quantities, so the elastic constants E and ν may be obtained from equations (2.1) and (2.2):

$$E = \frac{3F}{8aw_s} \qquad\qquad \nu = \sqrt{1 - \frac{3w_\infty}{4w_s}}\,. \tag{2.3}$$

These constants completely characterise the elastic behaviour of the tissue. To determine the fluid content of the tissue requires an analysis of the creep behaviour, this is carried out in the following subsection.

2.2 Fluid filled deformable porous media

Consider the problem depicted in Figure 6. A fluid filled porous media, of thickness l, is indented at the surface $z = 0$ by a cylindrical punch. Assuming that the elastic matrix is porous and incompressible and filled with an incompressible inviscid fluid, then conservation of mass leads to

$$\frac{\partial \phi^l}{\partial t} + \nabla \cdot (\phi^l \mathbf{v}^l) = 0 \tag{2.4}$$

$$\frac{\partial \phi^s}{\partial t} + \nabla \cdot (\phi^s \mathbf{v}^s) = 0\,, \tag{2.5}$$

where ϕ^α and $\mathbf{v}^\alpha$ denote the volume fraction and velocity of the liquid and solid phases. The sum of the two volume fractions is equal to one, hence, combining equations (2.4) and (2.5) gives

$$\nabla \cdot (\phi^l \mathbf{v}^l + \phi^s \mathbf{v}^s) = \mathbf{0} \,. \tag{2.6}$$

The momentum equations for each phase are

$$\begin{aligned} \nabla \cdot \underline{\underline{\sigma}}^s + K(\mathbf{v}^l - \mathbf{v}^s) &= \mathbf{0} & (2.7) \\ \nabla \cdot \underline{\underline{\sigma}}^l - K(\mathbf{v}^l - \mathbf{v}^s) &= \mathbf{0} \,, & (2.8) \end{aligned}$$

where K represents the drag coefficient between the solid and liquid, it is related to the solid permeability, κ, by $K = \phi^{l^2}/\kappa$ [11]. The stress tensors for each component are defined as

$$\begin{aligned} \underline{\underline{\sigma}}^s &= -(\phi^s p - \lambda e)\underline{\underline{I}} + 2\mu \underline{\underline{e}} & (2.9) \\ \underline{\underline{\sigma}}^l &= -\phi^l p \underline{\underline{I}} \,, & (2.10) \end{aligned}$$

where p is the fluid pressure and e is the trace of the strain tensor $\underline{\underline{e}}$. The Lamé constants, λ and μ should not be directly related to the elastic constants E, ν of the previous section. The standard definition relating the constants indicates that for an incompressible deformation, $\nu = 1/2$ and $\lambda = \infty$. In reality λ is modified from the elastic definition by the fluid pressure. For the current problem of indentation by a cylindrical punch the deformation is axisymmetric. In an axisymmetric system

$$e = \frac{\partial u}{\partial r} + \frac{u}{r} + \frac{\partial w}{\partial z} \,. \tag{2.11}$$

Summing the momentum equations and substituting for the stress tensors leads to

$$\nabla \cdot \left[(-p + \lambda e)\underline{\underline{I}} + 2\mu \underline{\underline{e}} \right] = \mathbf{0} \,. \tag{2.12}$$

To make progress consider the deformation near the centre of the contact, where $u, \frac{\partial}{\partial r} \to 0$ and $e \to \partial w/\partial z$. The deformation is then approximately one-dimensional. The one-dimensional form of equation (2.6) may be integrated to give

$$\phi^l \mathbf{v}^l{}_z + \phi^s \mathbf{v}^s{}_z = C(t) \,, \tag{2.13}$$

where the subscript z denotes the component in that direction. Near the base $z = l$ the deformation and velocities tend to zero, so $C(t) \equiv 0$. The solid velocity, $\mathbf{v}^s{}_z$, is simply the time derivative of the vertical displacement w, equation (2.13) then indicates that the fluid velocity is

$$\mathbf{v}^l{}_z = -\frac{\phi^s}{\phi^l} \frac{\partial w}{\partial t} \,. \tag{2.14}$$

The momentum equations may be written as

$$\begin{aligned} \frac{\partial}{\partial z}\left(-\phi^s p + (\lambda + 2\mu)\frac{\partial w}{\partial z} \right) - \frac{K}{\phi^l}\frac{\partial w}{\partial t} &= 0 & (2.15) \\ \frac{\partial}{\partial z}\left(-\phi^l p \right) + \frac{K}{\phi^l}\frac{\partial w}{\partial t} &= 0 \,. & (2.16) \end{aligned}$$

Summing these two equations provides a relation between the pressure and the deformation

$$-p + (\lambda + 2\mu)\frac{\partial w}{\partial z} = 0 \,. \tag{2.17}$$

Eliminating p from (2.15) and (2.16) leads to a diffusion equation for w

$$\frac{\partial w}{\partial t} = \Lambda \frac{\partial^2 w}{\partial z^2} , \tag{2.18}$$

where $\Lambda = \kappa(\lambda + 2\mu)$. This equation requires solving subject to one initial and two boundary conditions. At $t = 0$ the deformation is zero:

$$w(z, 0) = 0 . \tag{2.19}$$

At the substrate, $z = l$, the deformation is zero for all time:

$$w(l, t) = 0 . \tag{2.20}$$

As is standard with linear elasticity problems, the boundary condition at the top surface is applied on $z = 0$ for all time, even though the actual position of the surface varies. Assuming the force of the indenter is transmitted through the solid, normal to the surface, gives $\sigma^s_{zz} = F/\pi a^2$. Expanding this expression leads to the boundary condition at the top surface

$$-\phi_s p + (\lambda + 2\mu)\frac{\partial w}{\partial z} = \frac{F}{\pi a^2} . \tag{2.21}$$

Substituting for p from equation (2.17) reduces the final boundary condition to

$$\left.\frac{\partial w}{\partial z}\right|_{z=0} = \frac{F}{\pi a^2 \phi^l (\lambda + 2\mu)} = \Gamma . \tag{2.22}$$

The problem of evaluating the deformation in the vicinity of the centre-line is specified by (2.18) subject to conditions (2.19, 2.20, 2.22). The condition (2.22) involves the liquid volume fraction ϕ^l, which is an unknown function of z and t

$$\phi_l = 1 - \frac{\partial w}{\partial t} . \tag{2.23}$$

For simplicity, in the following ϕ^l will be set to a constant value, $\phi^l = \phi^l_0$, where ϕ^l_0 is the initial liquid volume fraction. The system in this case has a separable solution [12, page 113]:

$$w = \Gamma(z - l) - \frac{8\Gamma l}{\pi^2} \sum_{n=0}^{\infty} \frac{(-1)^n}{(2n+1)^2} \sin(\omega_n (z - l)) \exp(-r(2n+1)^2 t) , \tag{2.24}$$

where

$$\omega_n = (2n + 1)\frac{\pi}{2l} \qquad\qquad r = \frac{\Lambda \pi^2}{4l^2} .$$

For the present study the quantity of primary interest is the deformation of the top surface, $z = 0$, this is given by

$$w = -\Gamma l + \frac{8\Gamma l}{\pi^2} \sum_{n=0}^{\infty} \frac{1}{(2n+1)^2} \exp\left(-r(2n+1)^2 t\right) . \tag{2.25}$$

Clearly, as $t \to \infty$ the surface deformation $w(0) \to w_\infty$, so

$$w = w_\infty \left[1 - \frac{8}{\pi^2} \sum_{n=0}^{\infty} \frac{1}{(2n+1)^2} \exp\left(-r(2n+1)^2 t\right)\right] \tag{2.26}$$

and $w_\infty = \Gamma l$. Since w_∞ is known, equation (2.26) involves only one unknown, the decay rate r. The decay rate depends on the elastic constants, the fluid volume fraction, the indenter radius and the thickness of the tissue layer, it may be used to characterise the deformation. This will be an important indicator of the state of the tissue. It may be determined by fitting the curve specified by (2.26) to an experimental decay result.

2.3 Deformation of a viscoelastic solid

A number of authors have considered the consolidation of an indenter on a viscoelastic porous matrix, see [8, 13]. In [13] a closed form solution for the displacement due to a cylindrical indenter is given. However, the complexity of this solution, which involves the inverse Laplace transform of an infinite series of a number of integrals, is of little practical use. A more useful approach is to consider tissue as a simple viscoelastic material, see [14, 15] for example.

When the applied stress is fixed, the simplest approach to modelling a viscoelastic material is the Kelvin solid model. This represents the material as a spring and dashpot in parallel, in which case the stress-strain relation is

$$-\sigma_{ij} = E_v \epsilon_{ij} + \eta \frac{\partial \epsilon_{ij}}{\partial t} \ , \tag{2.27}$$

where E_v represents the elastic modulus of the solid and η represents the viscous response. The initial condition (2.19) indicates $\epsilon = 0$ at $t = 0$. The one-dimensional form of (2.27) may now be integrated to give

$$\epsilon = -\frac{F}{\pi a^2 E_v} \left(1 - \exp(-E_v t/\eta)\right) \ . \tag{2.28}$$

The deformation w is obtained by integrating the expression for ϵ,

$$w = -\frac{F}{\pi a^2 E_v} \left(1 - \exp(-E_v t/\eta)\right) (z - l) \ . \tag{2.29}$$

Finally, the surface deformation is

$$w = \frac{Fl}{\pi a^2 E_v} \left(1 - \exp(-E_v t/\eta)\right) = \frac{Fl}{\pi a^2 E_v} \left(1 - \exp(-r_v t)\right) \ . \tag{2.30}$$

As with the porous media solution, consideration of the large time behaviour allows the expression to be simplified

$$w = w_\infty \left(1 - \exp(-r_v t)\right) \ , \tag{2.31}$$

where, to be consistent with the previous section, the decay rate is denoted r_ν. So, again, the deformation may be characterised by a single constant.

2.4 Comparison with experimental results

So far, only one experimental result has been supplied. This involves a deformation with

$$a = 1\text{mm} \qquad F = 0.045\text{N} \qquad w_s = 1.1\text{mm} \qquad w_\infty = 1.4\text{mm},$$

the decay takes approximately 100ms. Values for the elastic constants may then be obtained from equation (2.3)

$$E = 1.2 \times 10^4 \text{Pa}, \qquad \nu = 0.2 \ .$$

Assuming the deformation is within 5% of its final value after 100ms indicates the appropriate decay rate is $r, r_\nu \approx 9$. Figure 7 shows a direct comparison of the deformations from the porous media model, (2.26), represented by the solid line and the viscoelastic solution, (2.31), represented by the broken line.

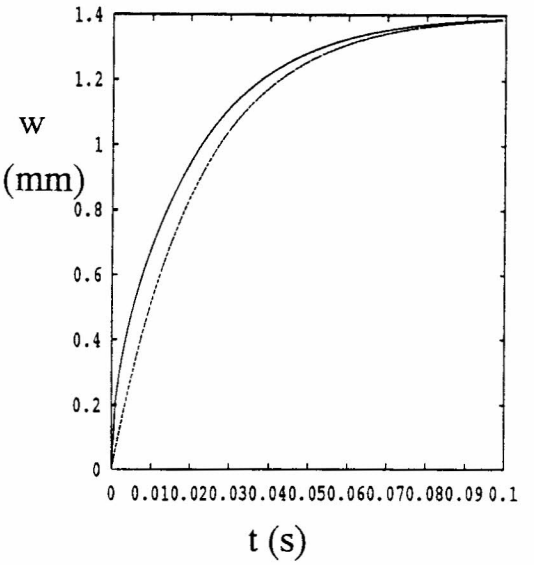

Figure 7: Comparison of the porous media and viscoelastic models.

2.5 Conclusions and recommendations

Assuming the fish freshness is characterised by its elasticity and fluid content, the analysis shows that the measurements made during the indentation phase are sufficient to characterise freshness with a reasonable degree of accuracy. The measurements required are the initial and final displacements and the time taken to reach the final displacement. The initial and final displacement of the indenter provides the elastic constants for the fish. These are defined by equation (2.3). The time taken to reach the final displacement gives the creep rate which provides information on the fluid content. This is obtained by comparing equation (2.26) or equation (2.31) with the experimental decay (it would appear that either of these solutions provide a sufficiently accurate representation of the deformation). A number of experiments should be carried out to accurately determine the correlation between these constants and the fish freshness.

Time constraints have prevented a thorough investigation of this problem. For this reason relatively simple model problems have been investigated. The pure elastic models presented are valid for an axisymmetric indenter on an elastic half-space. The porous media model is one-dimensional and valid on a strip of finite thickness, as is the viscoelastic solution. A reasonable comparison between the two configurations is strictly only possible if the diameter of the indenter is small and the thickness of the strip large. The porosity, ϕ_l, has been assumed constant to permit an analytical solution of the diffusion equation. A more accurate solution could be obtained by allowing ϕ_l to vary, the governing equation would then have to be solved numerically.

3 Models of phase C

We now consider models of the response of the fish when the probe's applied load is abruptly set to zero. See Figure 2.

3.1 A simple linear model of phase C

Assuming that the needle is in equlibrium at position $u = 0$ when the needle has no force applied, the simplest elastic response model for the needle is

$$Mu'' + ku' + \lambda u = h(t) \tag{3.1}$$

where

$$h(t) = 0 \quad \text{or} \quad h(t) = -F.$$

The initial displacement of the skin under this model is given simply by

$$u = -\Delta_1 = -F/\lambda. \tag{3.2}$$

From this we can estimate the elastic modulus of the skin of the fish by

$$\lambda = F/\Delta_1. \tag{3.3}$$

The probe as given has an aplied force of $F \approx 0.2N$ and with an observed displacement $\Delta_1 \approx 1\text{mm}$ we have

$$\lambda \approx 200\text{kg s}^{-2}. \tag{3.4}$$

A simple test of the model is to look at the output of the probe measurement and fit this to the model

$$u(t) = u_{mod}(t) \equiv ae^{-bt}\cos(ct + d). \tag{3.5}$$

Given experimental measurements $U(t_i)$ at times t_i the simplest way to do this is to solve the nonlinear optimisation problem

$$\min_{a,b,c,d} R(a,b,c,d) \equiv \sum_i |u_{mod}(t_i) - U(t_i)|^2. \tag{3.6}$$

This is a routine optimisation problem and was easily implemented using the MATLAB optimisation routines. The constants a, b, c and d then give information about the nature of the fish skin. The effectiveness of this procedure can be determined by seeing how large the minimum residual $R(a,b,c,d)$ is.

All attempts to implement this either did not converge or converged to a relatively large residual R. The model simply does not fit the data. An inspection of Figure 4 taken from the foam/plaice side also leads to this conclusion. Although the figure looks a bit like a damped cosine it is clear that after the initial peak (of height 1.45V) the first negative peak does not have a sinusoidal character and indeed is thinner than the next positive peak and of the same amplitude. A simple linear model can not reproduce this response.

3.2 A loss of contact model of phase C

An appealing modification to the simple elastic model of the upward motion of the probe is to consider the possibility that it might lose contact with the skin as it moves upwards, moves in free fall and then comes back into contact with the skin at a later time. This would seem to be consistent with the Figure 4. To test this hypothesis we returned to the foam experiment and this time glued the probe to the foam (using super glue). We considered that this would not affect its elastic properties significantly but would prevent loss of contact. To the eye (see Figure 8) the

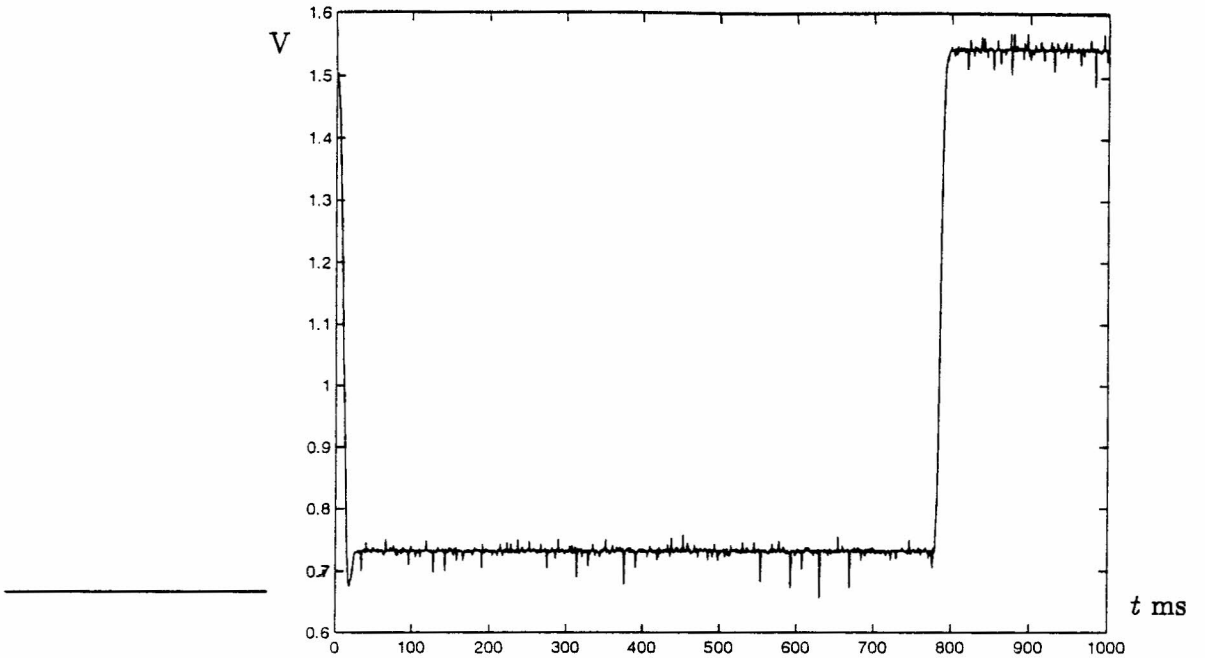

Figure 8: Output trace for foam when the probe was attached to the sample by superglue. Contrast with Figure 4.

results were different from the unglued model. We will look presently at applying signal processing to make this difference clearer.

To model the loss of contact we presume that during phase C (with no force applied) the probe has a mass M and as well as a damping force experiences an upwards force due to the reaction $R \geq 0$ from the skin. The skin is modelled to have a mass m and as well as moving under the force of the reaction with the probe also has an elastic restoring force $-\lambda u$ acting on it.

Skin and probe in contact
In this motion we have $R > 0$ and the skin and probe are both at the position $u(t)$. The equation of motion of the probe is then

$$Mu'' + k_1 u' = R - Mg \tag{3.7}$$

and of the skin is

$$mu'' + k_2 u' = -R - mg - \lambda u. \tag{3.8}$$

These two equations may be combined to give the simple linear elastic model of the last section given by

$$(M + m)\, u'' + (k_1 + k_2)\, u' + \lambda u = -\,(M = m)\, g. \tag{3.9}$$

When the probe and skin lose contact then $R = 0$ and they have respective motions $u_1(t) > u_2(t)$. The equation of motion of the probe is then

$$Mu_1'' + k_1 u_1' = -Mg, \tag{3.10}$$

and of the skin is

$$mu'' + k_2 u' = -R - mg - \lambda u. \tag{3.11}$$

Loss of contact occurs when $R = 0$ so that

$$Mu'' + k_1 u' + Mg = 0. \tag{3.12}$$

Substituting for u'' from (3.9) we have the *loss of contact condition*

$$(mk_1 - Mk_2)\, u' + \lambda M u = 0. \tag{3.13}$$

Loss of contact can also be monitored by measuring u_1''. If $R = 0$ and the probe is moving upwards we have

$$u'' = -g - k_1 u' < -g. \tag{3.14}$$

where we note that in terms of the units (volts) in which u_1 is measured we have

$$g = 9.8\text{ms}^{-2} = 9800\text{mm s}^{-2} = 7.84\text{kV s}^{-2}. \tag{3.15}$$

We note further that at loss of contact the function u'' is continuous, but unlike the simple linear model the function $u'''(t)$ is discontinuous.

Following loss of contact the skin moves elastically wheras the probe is in free fall. The independent motions can then be analysed. At some later time the probe and the skin will come back into contact again. We did not analyse this situation which is likely to be rather complex. It could be modelled by assuming that u, u' and u'' are continous at the second impact, but the situation may be rather more complex, with local skin deformations and even elastic waves playing a role. It is a worthy subject for further study. After the transient period of the probe and skin coming together they presumably move elastically again before a possible further loss of contact.

3.3 Experimental evidence for a loss of contact model

To compare the predictions of the loss of contact model with the actual measurements it was necessary to do some signal processing on the experimental data.

The experimental signal $U(t)$ was sampled at times t_i at $\delta t = 1$ ms time intervals. The resulting analogue samples $U(t_i)$ went through a 12 bit A/D convertor to give a set of recorded digital signals U_i. These signals all were rather noisy and required a measure of low pass filtering to reduce the noise component. We did this by using a simple 5 point moving average low pass filter to give the filtered signal $\bar{U}_i$. The resulting filtered signal was then differentiated twice using a simple $(-1, 0, 1)/\Delta t$ differentiating filter. Applying this once gives a discrete velocity V_i (see Figure 9) and twice gives a discrete acceleration A_i.

Interestingly a FFT analysis of A_i revealed a significant peak at a frequency of 100Hz, which is presumably the effect of mains on the measurements.

The values of A_i for the two cases of foam and 'glued foam' differed significantly, see Figures 10 and 11. In the case of unglued foam the acceleration (with the additional mains component) was smooth until it took a value of $-g$. At this point is became noisy and took a value close to $-g$ for a significant time interval. This seems to be compelling evidence for a loss of contact followed by free fall in which damping plays a role. There is some evidence also for a secondary loss of contact.

In the case of the glued foam the acceleration was smooth over a wide time interval and was $-g$ for only a short time. This is fully consistent with an elastic response over the whole interval.

It is worth noting that the measurement of the initial acceleration when the force is released gives us a second measure of the elastic modulus. From the model where both skin and probe are

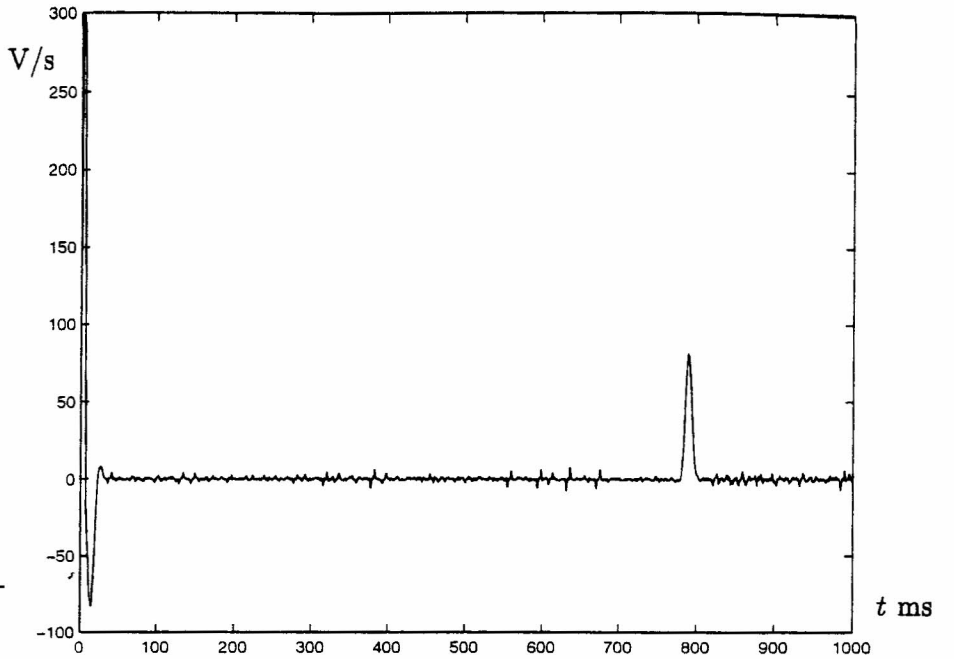

Figure 9: The first time derivative of the trace for foam, with the probe attached by glue.

in contact we can estimate that if Δ is the initial displacement below equilibrium then the initial acceleration when the force is released is given.by

$$u'' = -(M+m)/\Delta.$$

Hence

$$\lambda = -(M+m)/\Delta. \tag{3.16}$$

Now, the mass of the probe needle is 0.01kg, $\Delta \approx$ 1mm and from the measurements we have initially $u'' \approx 2 \times 10^4$ mms^{-2}. On the assumption that $m \ll M$ this gives

$$\lambda \approx 200\text{kg s}^{-2}$$

which is very similar to the previously calculated value.

We conclude from this section that

1. The motion of the skin and probe looks close to being linear
2. There is evidence for a subsequent loss of contact
3. After this there are further impacts (the probe behaves as an impact oscillator).

3.4 Multi-modal oscillators

It is unlikely that the fish skin will respoond as a simple elastic oscillator. When the probe meets the skin surface it indents it and the shape of this indent will be determined by the elastic response of a sheet - which will have many modes of response.

A simple model of this is to consider the skin to be modelled by four springs meeting at a central point with the probe attached to this central point. The group from Lancaster (Robin Tucker and Charles Wang) made some progress with this approach.

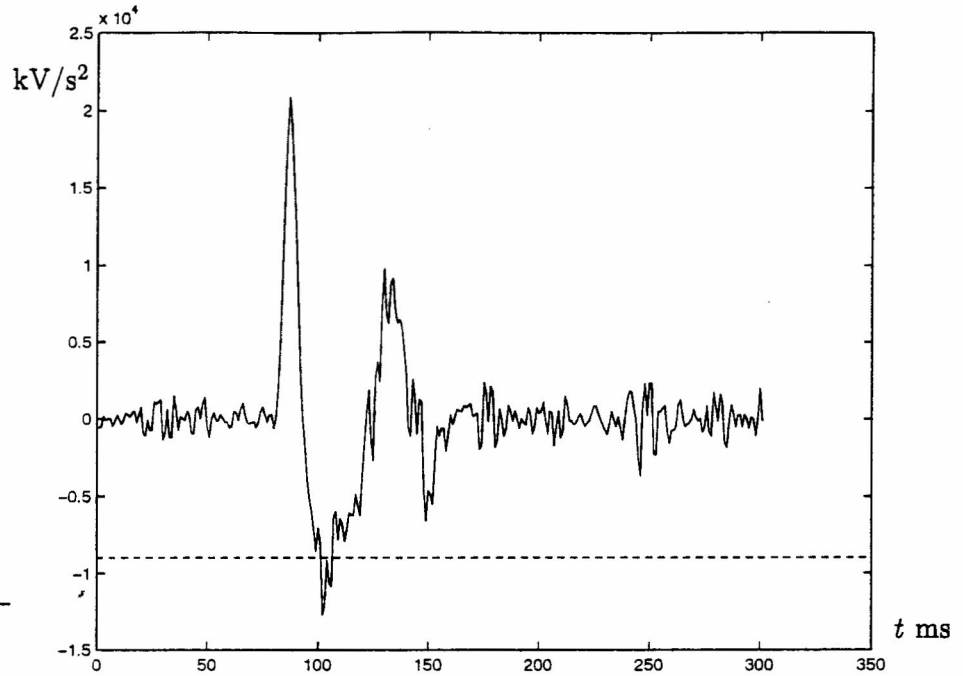

Figure 10: The second time derivative for the (unglued) foam sample. A horizontal line representing gravitational acceleration g has been added to the plot. (Phase C only shown.)

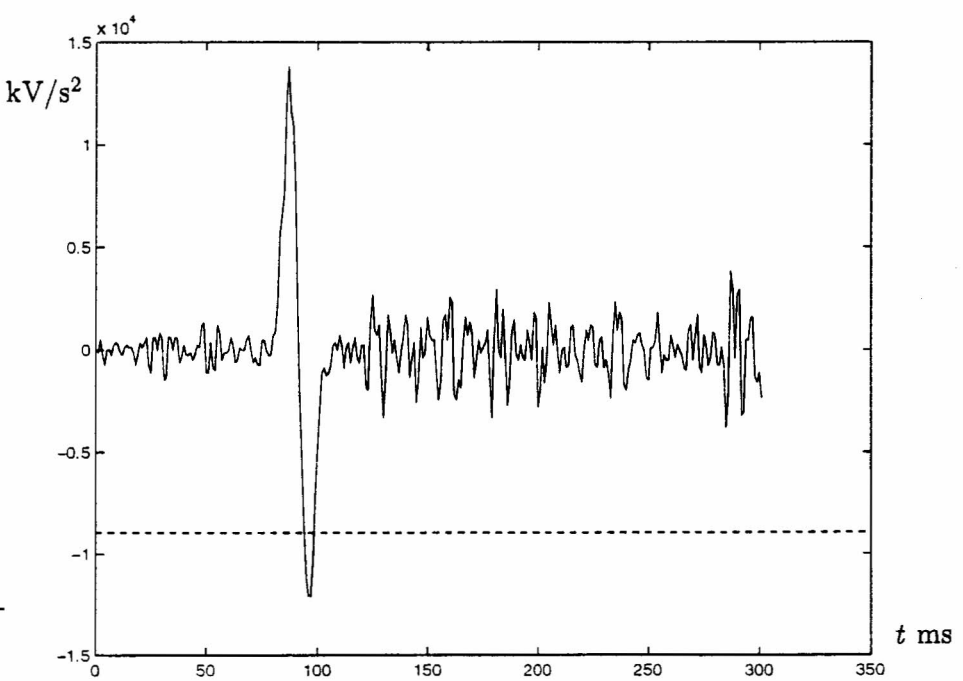

Figure 11: The second time derivative of the trace for foam, with the probe attached by glue. A horizontal line representing gravitational acceleration g has been added to the plot. (Phase C only shown.) Contrast with Figure 10.

4 Conclusions

- The probe is easy to use and it is also easy to extract data from it.
- Simple models lead to measures of the bulk elasticity and wetness of the fish.
- These need to be calibrated for different types of fish, but we note that the values seem to depend on which part of the fish are being used for measurement and how often the measurements are made (due to work hardening).
- More subtle models can be developed including impacts models, multi-modal and nonlinear models.

References

[1] C. Budd, *Can you tell a mathematician from a fish?*, address to the Royal Insitution of Great Britain, June 1999, on video.

[2] Suh J-K & Di Silvestro M.R. Biphasic poro-viscoelastic behaviour of hydrated biological soft tissue. Trans. ASMEJ. Appl. Mech. 66 pp528-535, 1999.

[3] Lai, W.M., J.S. Hou and V.C. Mow A triphasic theory for the swelling properties of hydrated charged soft biological tissues. *Biomechanics of Diarthrodial Joints Vol I.* Springer-Verlag, pp283-312 (1990).

[4] Mow V.C., Kuei S.C., Lai W.M. & Armstrong C.G. Biphasic creep and stress relaxation of articular cartilage in compression: Theory and experiment. ASME J. Biomech. Engng **102** pp73-84 (1980).

[5] Barry S.I. Flow in a deformable porous medium. Ph.D. Thesis, Australian Defence Force Academy (1990).

[6] Terzhagi K. Erdbaumechanik auf Boden Physikalischer Grundlage. F. Deuticke, Vienna (1925).

[7] Biot M.A. General theory of three-dimensional consolidation. J. Appl. Phys. **12** pp155-164 (1941).

[8] Chiarella C. & Booker J.R. The time-settlement behaviour of a rigid die resting on a deep clay layer. Q. Jl. Mech. Appl. Math 28(3) pp317-328 1975.

[9] Davis E.H. & Poulos H.G. 4th Aust. N.Z. Conf. Soil Mech. pp233- 1963.

[10] Johnson K.L. Contact Mechanics. CUP 1985.

[11] Lai W.M. & Mow V.C. Drag induced compression of articular cartilage during a permeation experiment. Biorheology 17, pp111-123 1980.

[12] Carslaw H.S. & Jaeger J.C. Conduction of heat in solids. Oxford Sci. Publ. 2nd Ed. 1959.

[13] Szefer G. & Gaszyński J. Axisymmetric punch problem under condition of consolidation. Archives of Mechanics 27(3)pp497-515 1975.

[14] Fung Y.C. Foundations of solid mechanics. Prentice-Hall 1965.

[15] Chung T.J. Continuum mechanics. Prentice-Hall 1988.